[CANCER RESEARCH 64, 5913–5919, September 1, 2004]

Advances in Brief

A Missense Mutation in KIT Kinase Domain 1 Correlates with Imatinib Resistance in Gastrointestinal Stromal Tumors

Lei L. Chen,[1] Jonathan C. Trent,[1] Elsie F. Wu,[2] Gregory N. Fuller,[3] Latha Ramdas,[3] Wei Zhang,[3] Austin K. Raymond,[3] Victor G. Prieto,[3] Caroline O. Oyedeji,[1] Kelly K. Hunt,[4] Raphael E. Pollock,[4] Barry W. Feig,[4] Kimberly J. Hayes,[5] Haesun Choi,[6] Homer A. Macapinlac,[7] Walter Hittelman,[8] Marco A. Velasco,[9] Shreyaskumar Patel,[1] Michael A. Burgess,[1] Robert S. Benjamin,[1] and Marsha L. Frazier[2]

Departments of [1]Sarcoma, [2]Epidemiology, [3]Pathology, [4]Surgery, [5]Cytogenetics, [6]Diagnostic Radiology, and [7]Nuclear Medicine, [8]Experimental Therapeutics, The University of Texas M. D. Anderson Cancer Center, Houston, Texas; and [9]Vel-Lab Research, Houston, Texas

Abstract

KIT gain of function mutations play an important role in the pathogenesis of gastrointestinal stromal tumors (GISTs). Imatinib is a selective tyrosine kinase inhibitor of ABL, platelet-derived growth factor receptor (PDGFR), and KIT and represents a new paradigm of targeted therapy against GISTs. Here we report for the first time that, after imatinib treatment, an additional specific and novel KIT mutation occurs in GISTs as they develop resistance to the drug. We studied 12 GIST patients with initial near-complete response to imatinib. Seven harbored mutations in KIT exon 11, and 5 harbored mutations in exon 9. Within 31 months, six imatinib-resistant rapidly progressive peritoneal implants (metastatic foci) developed in five patients. Quiescent residual GISTs persisted in seven patients. All six rapidly progressive imatinib-resistant implants from five patients show an identical novel *KIT* missense mutation, 1982T→C, that resulted in Val654Ala in KIT tyrosine kinase domain 1. This novel mutation has never been reported before, is not present in pre-imatinib or post-imatinib residual quiescent GISTs, and is strongly correlated with imatinib resistance. Allelic-specific sequencing data show that this new mutation occurs in the allele that harbors original activation mutation of *KIT*.

Introduction

Gastrointestinal stromal tumors (GISTs) originate from transformation of interstitial cells of Cajal, a network of innervated cells that coordinate peristalsis in the gastrointestinal system. Aberrant KIT signals represent the initiating event in the pathogenesis of GISTs and *KIT* gain of function mutations have been reported (1–3). Microarray analysis showed that GISTs exhibit a remarkably homogeneous gene expression profile unlike the extremely heterogeneous patterns seen in common epithelial cancers (4). KIT with an exon 11 mutation that replaced Lys558 with Val (Lys558Val) was introduced by knock-in strategy, and this produced tumors indistinguishable from human GISTs (5). These results indicate that constitutive KIT signaling is both critical and sufficient for GIST.

The locations of *KIT* mutations are nonrandom and vary according to cell lineage. *KIT* exon 11 is the most frequent mutation site for GISTs (1, 2), most commonly clustered in cytoplasmic juxtamembrane region between 550 and 563, resulting in pathological release from autoinhibition (6, 7) and constitutive activation of KIT. Mutations in exon 9 make up 3 to 21% of all cases. Mutation in exon 13 is rare; to date, there are only five reported cases (2, 8), all exhibiting the same 1945A→G, Glu642Lys mutation, which is 12 amino acids NH_2-terminal to the novel mutation reported here. Exon 17 mutation is extremely rare in GISTs, with only three reported cases thus far: two sporadic cases with Asn822His and Asn822Lys (3) and one Asp820Tyr mutation in a patient with familial GIST with dysphagia (9). GISTs with wild-type KIT range from 3 to 35% of cases and often have platelet-derived growth factor receptor (PDGFR) α activating mutation (3, 10, 11). Imatinib (gleevec, STI571; refs. 12, 13) is a selective ATP-competitive inhibitor of KIT, BCR-ABL, and PDGFRα and β and is the only drug effective against GISTs (3, 14, 15). Imatinib revolutionized the care of GIST patients and represents a new paradigm of targeted cancer chemotherapy. Unfortunately, imatinib resistance has begun to emerge. Elucidation of drug resistance mechanism should provide new insights in reversing drug resistance and the discovery of new targets for cancer therapy.

GIST patients often present with liver metastases and peritoneal implants. Each individual peritoneal implant can be viewed as a single clone growing *in vivo*, that can be monitored clinically by computed tomography scan and positron emission tomography (PET) scan and on which intervention by surgery or biopsy can be done at the onset of radiographic progression. Each clinical phase of disease and tumor evolution can be correlated with specific molecular events. Taking advantage of the unique features of GISTs, we report here a novel *KIT* mutation in exon 13 that correlates with the emergence of imatinib resistance and rapid progression in GISTs.

Materials and Methods

Patient and Clinical Trials. Ten patients participated in Institutional Review Board (IRB)-approved phase III randomized intergroup trial S00–33; two patients were treated with imatinib off protocol after the S00–33 intergroup trial was closed. All of the patients took imatinib until the day of surgery, and tumor specimens were obtained with consent on IRB- approved laboratory trial LAB02–433.

Cytogenetic Analyses. Conventional cytogenetic analysis was done on primary GIST cells from patient A, Clones 1 and 2 after 72–96 h of culture. Twenty metaphases were analyzed.

Genomic DNA and cDNA Sequence Analysis of *KIT*. DNA was isolated from paraffin-embedded or frozen tissue or from peripheral blood mononuclear cells (PBMCs) by using a QIAamp DNA minikit (Qiagen Inc., Valencia, CA) according to the manufacturer's instructions. RNA was extracted from frozen tissue by standard methods and by using a RNeasy minicolumn according to the manufacturer's instructions (Qiagen Inc.). The cDNA was prepared by using Two-step Taqman Reverse Transcription reagent (Applied Biosystems, Foster City, CA) according to the manufacturer's instructions, except that, instead of using random primers, a primer specific for *KIT* RNA was used (*KIT* 2961R, 5′-TTCCTGGAGGGGTGACCCAAACACT). The cDNA was

Received 1/11/04; revised 6/15/04; accepted 7/13/04.

Grant support: Funding from Division of Cancer Medicine, National Cancer Institute (NCI) grant CA16672 (supporting the DNA Sequencing Core Facility, Nucleic Acid Extraction Facility, and Tissue Procurement and Banking Facility), NCI contracts U01-CA70172-01, N0-CM-17003, at University of Texas, M. D. Anderson Cancer Center and Goodwin Foundation.

The costs of publication of this article were defrayed in part by the payment of page charges. This article must therefore be hereby marked *advertisement* in accordance with 18 U.S.C. Section 1734 solely to indicate this fact.

Requests for reprints: Lei L. Chen, Department of Sarcoma (Unit 450), The University of Texas M. D. Anderson Cancer Center, 1515 Holcombe Boulevard, Houston, Texas 77030. Phone: 713-792-3626; Fax: 7130-794-1934; E-mail: llchen@ mdanderson.org.

Table 1 *Primer sequence*

No.	Type	Primer sequence	Codon, region in KIT
1	Genomic	F: 5′-CCCAAGTGTTTTATGTATTT R: 5′-ATGGTGTGATGCATGTATTA	449–514, exon 9
2	Genomic	F: 5′-TCCAGAGTGCTCTAATGAC R: 5′-AGGTGGAACAAAACAAAGG	550–591, exon 11
3	Genomic	F: 5′-TACTGCATGCGCTTGACATC R: 5′-CCAAGCAGTTTATAATCTAGC	627–664, exon 13
4	Genomic	F: 5′-TTCTACATGTCCCACTTGATT R: 5′-AGCATGATATACATACTCTCTG	715–744, exon 15
5	Genomic	F: 5′-GTGAACATCATTCAAGGCGT R: 5′-CCTTTGCAGGACTGTCAAGCA	788–828, exon 17
6	cDNA	F: 1265: 5′-TCCTGACTTACGACAGGCTCGT R: 1611: 5′-ACATCATGCCAGCTACGATT	409–524, extracellular + TM
7	cDNA	F: 1577: 5′-ACACCCTGTTCACTCCTTTGCTGA R: 2136: 5′-GACTCCTTTGAATGCAGAAGA	519–706, TM + kinase I
8	cDNA	F: 2071: 5′-CGTGATTCATTTATTTGTTC R: 2510: 5′-CATCCACTTCACAGGTAGTC	684–830, kinase insert + kinase 2
9	cDNA	F: 2387: 5′-TTCACAGAGACTTGGCAGCCAG R: 2961: 5′-TCCTGGAGGGGTGACCCAAACACT	789–976, kinase 2 + COOH-terminal

Abbreviations: F, forward; R, reverse; TM, transmembrane.

then subjected to PCR. Nucleotide sequencing was analyzed with a 3730 × 1 DNA Analyzer from Applied Biosystems at the M. D. Anderson Cancer Center Nucleic Acid Core Facility. The Genomic DNA sequence of exons 9, 11, 13, 15, and 17 was analyzed (primers 1–5; Table 1) in all GIST specimens, pre-imatinib GISTs, and PBMCs. RNA was extracted from all of the surgical specimens. Taking into consideration the alternative splicing sites (16) and the hot spots of KIT mutation, we designed primers (Table 1, primers 6–9) to sequence the cDNA encompassing exons 9 to 21.

Allelic-specific cDNA Sequence. We used restriction endonuclease *Bse*RI (New England BioLabs Inc., Beverly, MA) to preferentially digest the PCR product of the normal allele but spared the mutated allele of clone 5 of patient C. The digested DNA fragments were separated by agarose gel electrophoresis, eluted from the gel, and sequenced. We used an alternative PCR method with mutation-specific primers to preferentially amplify the mutated allele for sequencing. We also sequenced the counterpart normal allele for comparison.

Results

Patients and Clinical Course. The clinical course of GIST patients varies. Most patients continue to enjoy remission, but a small percentage of GIST patients who had initial near-complete response subsequently showed mixed response with the emergence of new liver lesion(s) or rapidly progressing imatinib-resistant implant(s), although the rest of implants and or liver metastases remained responsive to imatinib. At the present time, among approximately 130 patients, we have identified five patients who unequivocally developed imatinib resistance under close surveillance by radiographic criteria and were amenable for biopsy or surgical resection of the resistant implants, and all five patients (designated as patients A–E, Table 2) were included in this study. Some GIST patients had initial near-complete remission

Table 2 *KIT sequence of pre-imatinib, post-imatinib residual GISTs, and clones 1–11*

Patients (A-L) and characteristics of GIST specimens	*KIT* sequence		
	Exon 11*	Exon 9†	Exon 13
Patient A			
Pre-imatinib	1690T→G	Normal	Normal
Clone 1, rapid progression	1690T→G	Normal	1982T→C (Val654Ala)
Clone 2, rapid progression	1690T→G	Normal	1982T→C (Val654Ala)
Clone 3, stable/quiescent	1690T→G	Normal	Normal
Patient B			
Pre-Imatinib	1691–1696del6	Normal	Normal
Clone 4, rapid progression	1691–1696del6	Normal	1982T→C (Val654Ala)
Patient C			
Pre-imatinib	1694–1708del15	Normal	Normal
Clone 5, rapid progression	1694–1708del15	Normal	1982T→C (Val654Ala)
Clone 6, stable/quiescent	1694–1708del15	Normal	Normal
Clone 7, stable/quiescent	1694–1708del15	Normal	Normal
Patient D			
Pre-imatinib	1690–1695del6	Normal	Normal
Clone 8, rapid progression	1690–1695del6	Normal	1982T→C (Val654Ala)
Clone 9, stable/quiescent	1690–1695del6	Normal	Normal
Patient E			
Clone 10, pre-imatinib	Normal	1525–1530ins6	Normal
Clone 11, rapid progression	Normal	1525–1530ins6	1982T→C (Val654Ala)
Patients F,G,H,I			
Residual, stable/quiescent	Normal	1525–1530ins6	Normal
Patient J			
Residual, stable/quiescent	1697T→G	Normal	Normal
Patient K			
Residual, stable/quiescent	1697–1708del12	Normal	Normal
Patient L			
Residual, stable/quiescent	1700T→G	Normal	Normal

Abbreviations: del, deletion; ins: insertion.

* Exon 11: 1690T→G ⇒ Try557Gly; 1691–1696del ⇒ TryLys$^{557–558}$ deletion plus Val559Phe; 1694–1708del ⇒ LysValVal GluGlu$^{558–562}$ deletion; 1690–1695del ⇒ TryLys$^{557–558}$ deletion; 1697T→G ⇒ Val559Gly; 1697–1708del ⇒ ValVal GluGlu$^{559–562}$ deletion; 1700T→G ⇒ Val560Gly.

† Exon 9: 1525–1530ins ⇒ AlaTyr$^{502–503}$ tandem repeat.

followed by a plateau showing persistent stable residual tumor. We have identified seven such patients who were amenable for surgical resection of the residual quiescent GISTs, and all seven patients (designated as patients F–L, Table 2) were included in this study. Except for patients C and F, 10 patients participated in the S00–33 intergroup trial, and all were randomized to the imatinib 400-mg/d arm. All 12 patients were treated with 400 mg imatinib per day.

The pre-imatinib computed tomography scan of patient A revealed multiple single and matted peritoneal implants in the patient's abdomen (Fig. 1*a-1*) and pelvis (Fig. 1*a-2*). Patient A had a swift excellent response with near-total resolution of GISTs and marked reduction of abdominal girth within 8 weeks of imatinib treatment (Fig. 1*a-3, a-4*). PET scans showed initial multiple hypermetabolic tumor implants followed by near-total resolution of all hypermetabolic activities 8 weeks after imatinib therapy (Fig. 1*a-7, a-8*). Patient A continued to respond to imatinib until 28 months later, when a small new implant appeared in the small bowel mesentery and progressed rapidly within 3 months (Fig. 1*a-5, clone 1*). Subsequently, a second small implant (clone 2) became visible on computed tomography scan (Fig. 1*a-6, clone 2*). PET computed tomography scan revealed two discrete small areas of intense hypermetabolic tumor (Fig. *1a-9, a-10, yellow spots indicated by arrows*) that corresponded to clones 1 and 2, respectively. The doubling time of clone 1 was calculated to be 35 days. Intra-operatively, clones 1 and 2 were found to be purple-brownish vascular viable tumor implants and were surgically removed. What came as a surprise was the finding that there were more than 200 small white, soft, quiescent appearing nodules found throughout patient A's abdomen and pelvis, not readily visible on computed tomography scans. Complete debulking was not possible; a representative specimen was removed for diagnosis and is designated as clone 3 (Table 2). These quiescent nodules showed extensive treatment effect with very small areas of viable GIST cells seen on histologic examination. Within 8 weeks of imatinib treatment, most of GISTs resolved, but small pockets of cells escaped apoptosis, remained quiescent, and survived for more than 2 years in patient A.

Patient B presented with multiple liver metastases and single and matted peritoneal implants, some coalescing into large masses (Fig. 1*b-1*). computed tomography scans 8 weeks (data not shown) and 4 months after imatinib treatment (Fig. 1*b-2*) were very similar and showed near-total resolution of all implants and the appearance of hypoattenuating liver lesions, which indicated necrosis and a good response to treatment. A new implant (Fig. 1*b-3, arrow, clone 4*) appeared 6 months after imatinib treatment and was visible as a tiny implant between the spleen and the contrast-filled stomach. Within 3 months, clone 4 progressed into a huge implant (Fig. 1*b-4, arrow*) with an estimated doubling time of 10 days. All other implants and liver lesions remained sensitive to imatinib. Complete resection of clone 4 was not possible and biopsy was done.

Patient C presented with multiple implants in left upper quadrant, one of which bore a surgical clip (Fig. 1*c-1, a dense white tiny rod at 4 o'clock*) and which can be identified and traced to an implant much reduced in size, 8 weeks post imatinib (Fig. 1*c-2, a tiny dense white dot at 3 o'clock*). Nineteen months later a small implant was noted (Fig. 1*c-3, short arrow, clone 5*), which was not present in previous computed tomography scans done at 8 weeks or 16 months post-imatinib treatment and which represented an imatinib-resistant implant with rapid progression (Fig. 1*c-4, arrow, clone 5*). Two quiescent nodules from omentum were also removed and are designated as clones 6 and 7 (Table 2). Patient D had initial excellent response, as shown in Fig. 1-*D-1* and *-D-2*, and developed a small new implant (Fig. 1*d-3, arrow, clone 8*) 19 months after imatinib treatment; this implant progressed rapidly within 4 months (Fig. 1d-4, arrow, clone 8). Patient E developed imatinib-resistant, rapidly growing implants 31 months after imatinib treatment (computed tomography scans not shown). Patients C, D, and E underwent surgery immediately at the onset of imatinib resistance, and clones 5–11 (Table 2) were surgically removed from these three patients.

Patients F–L underwent surgical resection of stable/quiescent residual GISTs at the time when the response to imatinib reached plateau.

***KIT* Mutation Before Imatinib Treatment.** We did direct sequencing of *KIT* genomic DNA (exons 9, 11, 13, 15, 17) on all GISTs, including paraffin-embedded specimens. Direct sequencing of cDNA was done on clones 1–11 and on all surgical and biopsy specimens of GISTs. The results of *KIT* mutations, deletions (del) and insertion (ins) of all 12 patients are summarized in Table 2. The corresponding amino acids changes in KIT are listed in a footnote of Table 2. The initiating events that cause constitutively active KIT of patients A–D and J–L involved different mutation sites in exon 11 (ranging from nucleotides 1690 through 1708) resulting in amino acid changes (ranging from Try557 to Glu562) in cytoplasmic juxtamembrane region. Patients E–I showed a 6-bp insertion in exon 9 that resulted in a tandem repeat of AlaTyr (502–503) in extracellular juxtamembrane region.

Development of a New Missense Mutation in KIT Kinase Domain 1 Is Correlated with the Emergence of Imatinib Resistance in GISTs After Initial Excellent Response. Most strikingly, all six imatinib-resistant rapidly growing clones [clones 1, 2, 4, 5, and 8 (Fig. 1, *arrows*) and clone 11 (computed tomogram not shown)] from five patients (patients A–E) showed an identical novel exon-13 missense mutation, 1982T→C (Fig. 2*c*, *d*, and *f*; Table 2), resulting in a substitution of Val by Ala at codon 654 (Val654Ala) in tyrosine kinase domain 1 of KIT (Fig. 3). This new mutation has never been reported in literature before and is not found in any pre-imatinib GISTs (Fig. 2*a* and *e*; Table 2) of any of the 12 patients nor in any of the residual quiescent clones [clones 3 (Fig. 2*b*), 6, 7, or 9], nor in any residual stable quiescent post-imatinib GISTs from patients F–L, nor on the PBMCs of patients A–E (data not shown). Both genomic and cDNA sequence in both forward and reverse directions were done to confirm this new mutation. Because this novel exon 13 mutation, identified in imatinib-resistant, rapidly growing clones 1, 2, 4, 5, 8, and 11 from patients A–E, are identical, we showed the chromatograms of patients A and B only (Fig. 2). These data indicate that this novel 1982T→C missense mutation is nonrandom and is strongly correlated with imatinib resistance and rapid progression of GIST.

Allelic-specific Sequence Analyses Demonstrate the Occurrence of the Novel 1982T→C Missense Mutation in the Original Mutated Allele. The 1982T→C mutation is heterozygous as shown in Fig. 2. Allelic-specific sequence analyses were done to determine whether this second event of 1982T→C mutation in KIT occurs in the wild-type or the original mutated allele that bears the dominant activation exon 11 or exon 9 mutation. Clone 5 from patient C shows a 15-bp deletion in exon 11 (Table 2). This deleted 15-bp (1694–1708, AGGTTGTGAGGAGA), interestingly, contains the unique restriction endonuclease *Bse*RI recognition site, GAGGAG. We used primer 7 (Table 1) and PCR to generate cDNA that encompass exon 10–14. A 579-bp (wild-type allele) and a 564-bp (1694–1708del15) cDNA were generated. Restriction endonuclease mapping shows that *Bse*RI will cut the wild-type 579-bp DNA only once and will spare the 564-bp cDNA that is devoid of the *Bse*RI recognition site. An example of *Bse*RI partial digestion followed by agarose gel electrophoresis (2%) is shown in Fig. 4*A*. Four bands including a 579-bp (*top band*) undigested normal allele, a 564-bp undigested cDNA from mutated allele, a 125-bp 5′ end of digested fragment and a 454-bp 3′ end of digested fragment (containing exon 13) from normal allele can be visualized. On complete digestion by *Bse*RI, the 579-bp DNA became completely digested and only three bands can be visualized. Direct

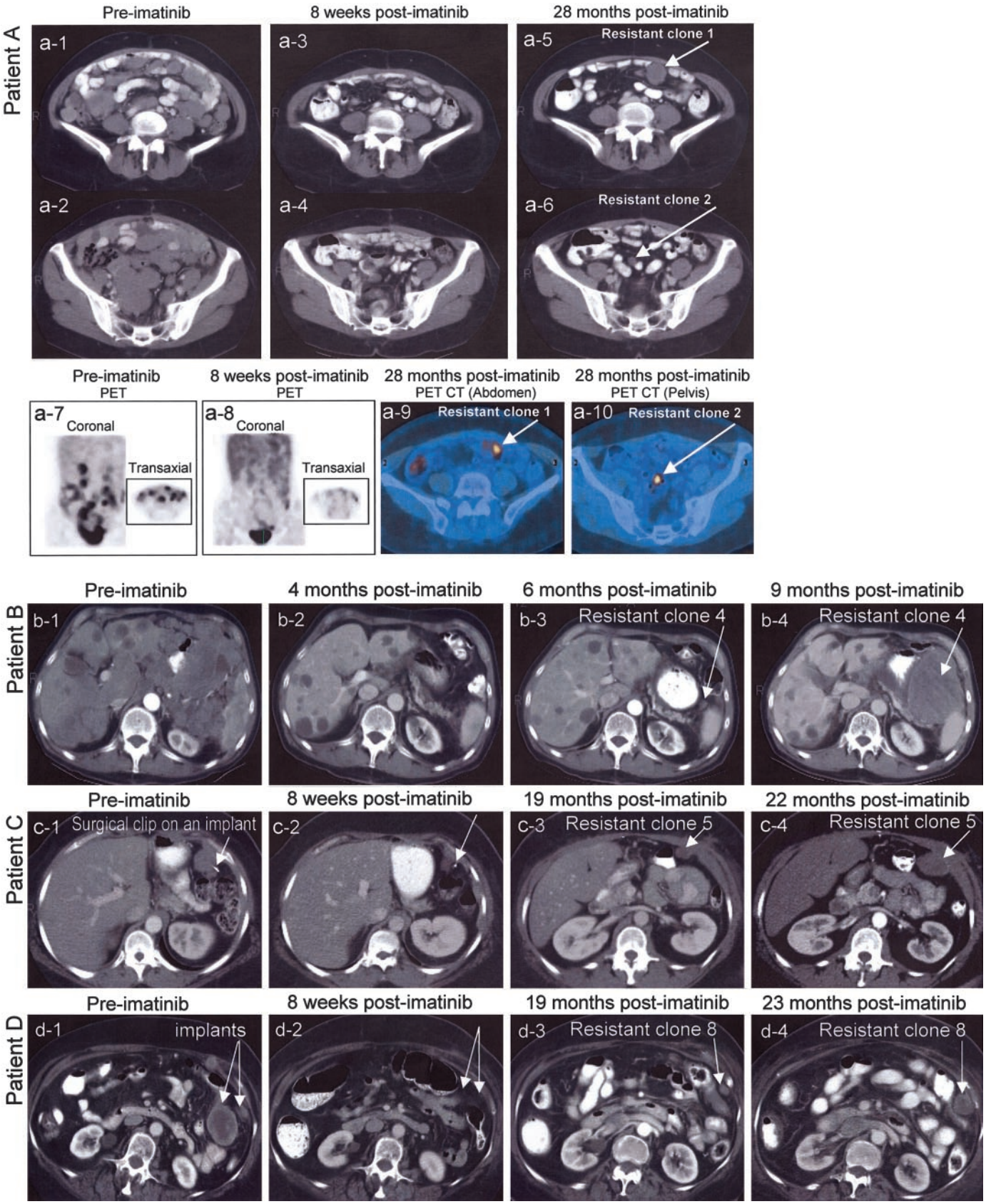

Fig. 1. Computed tomography (*CT*), PET, and PET CT scan images of patient A (*a-1 to a-10*), patient B (*b-1 to b-4*), patient C (*c-1 to c-4*), and patient D (*d-1 to d-4*). *a-1* and *a-2*, pre-imatinib CT images of patient A showing multiple peritoneal tumor implants. *a-3* and *a-4*, CT images obtained at 8 weeks post-imatinib treatment, demonstrating rapid resolution of most of peritoneal tumor implants. *a-5* and *a-6*, CT images 28 months post-imatinib treatment demonstrating two new imatinib-resistant implants in the small bowel mesentery (*arrows*, *a-5*, *clone 1*; *a-6*, *clone 2*). *a-7*, pre-imatinib PET showing multiple hypermetabolic tumor implants. *a-8*, PET images 8 weeks post-imatinib treatment demonstrating near-total resolution of all hypermetabolic tumors. In *a-9* and *a-10*, PET CT 28 months post-imatinib treatment revealed two new discrete hypermetabolic tumor implants (*two yellow spots*, *arrows*), correspond to the resistant clone 1 (*arrow*) and clone 2 (*arrow*). *b-1*, pre-imatinib CT images of patient B showing multiple liver metastases and matted peritoneal implants. *b-2*, CT of abdomen obtained 4 months after imatinib treatment showing near-total resolution of all implants and hypoattenuating liver lesions, indicating necrosis or good

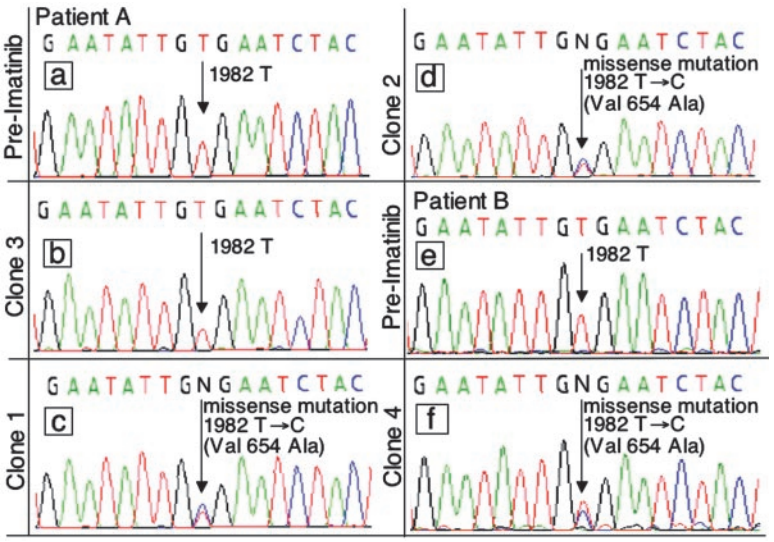

Fig. 2. The chromatograms of *KIT* mutation of patient A (*a–d*) and patient B (*e* and *f*) demonstrate that a novel missense mutation in *KIT* exon 13 correlates with imatinib-resistant rapid progression of GISTs. *a*, genomic DNA sequence from pre-imatinib GIST of patient A, showing the wild-type 1982T. *b*, genomic DNA sequence from the residual quiescent clone 3, showing wild-type 1982T. *c*, genomic DNA sequence from the imatinib-resistant rapidly growing clone 1, showing a new missense mutation, 1982T→C, resulting in Val654Ala. *d*, genomic DNA sequence from the imatinib-resistant rapidly growing clone 2, showing the same new 1982T→C mutation. *e*, genomic DNA sequence from pre-imatinib GIST of patient B showing wild-type 1982T. *f*, genomic DNA sequence from imatinib-resistant rapidly growing clone 4, showing the same new 1982T→C mutation.

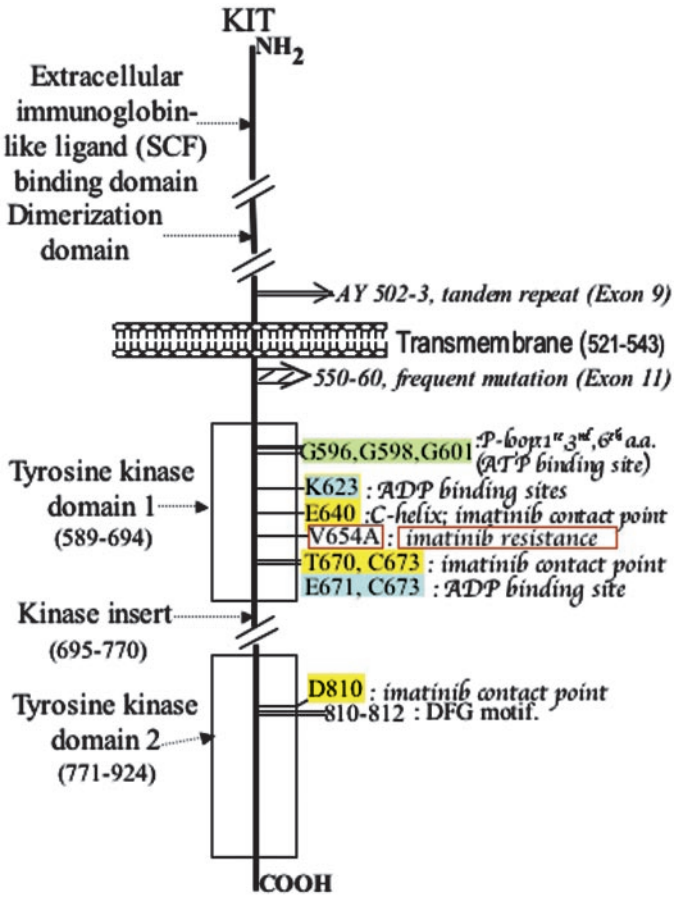

Fig. 3. Structural and functional regions of KIT. *Yellow highlight*, imatinib contact points; *green*, KIT ATP phosphate-binding loop (*P-loop*); *blue*, ADP binding sites; *red box*, Val654Ala mutation. (*SCF*, stem cell factor)

sequencing of DNA eluted from these four bands were done (the sequences are shown in Fig. 4*B*). Figure 4*B* (*upper left panel*) shows that the 579-bp DNA, which represents the undigested normal allele, exhibits a wild-type exon 11 sequence with the intact *Bse*RI recognition site, GAGGAG. Figure 4*B* (*the lower panel*) shows that the undigested 564-bp DNA, which was derived from the original mutated allele, contain both the 15-bp deletion and the 1982T→C mutation. The 454-bp 3′ end fragment, derived from normal allele DNA, shows wild-type 1982T (Fig. 4*B*, *top right panel*). For patients A, B, D, and E, we used mutation-specific primers to selectively PCR-amplify the mutated allele for sequencing. The normal allele counterparts were also examined for comparison. We found the second exon 13 (1982T→C) mutation in the original mutated allele in all six of the imatinib-resistant clones in all five of the GIST patients.

Histology and Cytogenetics. There is no distinguishable difference in histology between the imatinib-resistant clones and the pre-imatinib GIST (data not shown). We analyzed 20 metaphase GIST cells from each of clones 1 and 2 and found that their karyotypes were normal (data not shown). There was no cytogenetic evidence to suggest amplification of the multidrug resistance or *KIT* genes.

Discussion

This is the first report of a strong association between rapidly progressive imatinib-resistant GIST after initial near-complete response to treatment and mutation in KIT kinase domain 1. In leukemia, the imatinib-resistant clones are mixed with imatinib-sensitive clones and normal bone marrow and blood, whereas, in GIST, individual implants are distinct (Fig. 1) and can be closely monitored by computed tomography and PET scans, so that immediate biopsy or surgical removal of specific imatinib-resistant clones is possible. This unique feature provides convincing evidence for the temporal relationship between the emergence of resistance *in vivo* and evolution of this new *KIT* mutation, Val654Ala, in exon 13. In comparison with leukemia, GIST is a relatively slow-growing tumor without excessive chromosome instability. To date, no untreated GISTs have been

response. *b-3* and *b-4*, CT of abdomen, 6 and 9 months post-imatinib treatment, respectively. A suspicious tiny implant (*b-3*, *arrow*, *Resistant clone 4*) was noted between spleen and stomach. Rapid progression of clone 4 (*arrow*, *b-4*) was noted within 3 months. *c-1* and *c-2*, CT scans of patient C pre-imatinib and 8 weeks post- imatinib, respectively. One of the implants (*patient's left upper quadrant*, *c-1*) bears a surgical clip that can be identified and traced to an implant that is much reduced in size 8 weeks post-imatinib (*c-2*). *c-3* and *c-4*, 19 months later, a small implant was noted (*c-3*, *short arrow*, *clone 5*) that was not present in previous CT scans done at 8 weeks or 16 months post-imatinib treatment and that represented an imatinib-resistant implant with rapid progression (*c-4*, *arrow*, *clone 5*). *d-1* and *d-2*, CT scans of patient D show initial excellent response. *d-3* and *d-4*, rapid progression of a tiny tumor implant (*arrow*, *Resistant clone 8*) in the omentum.

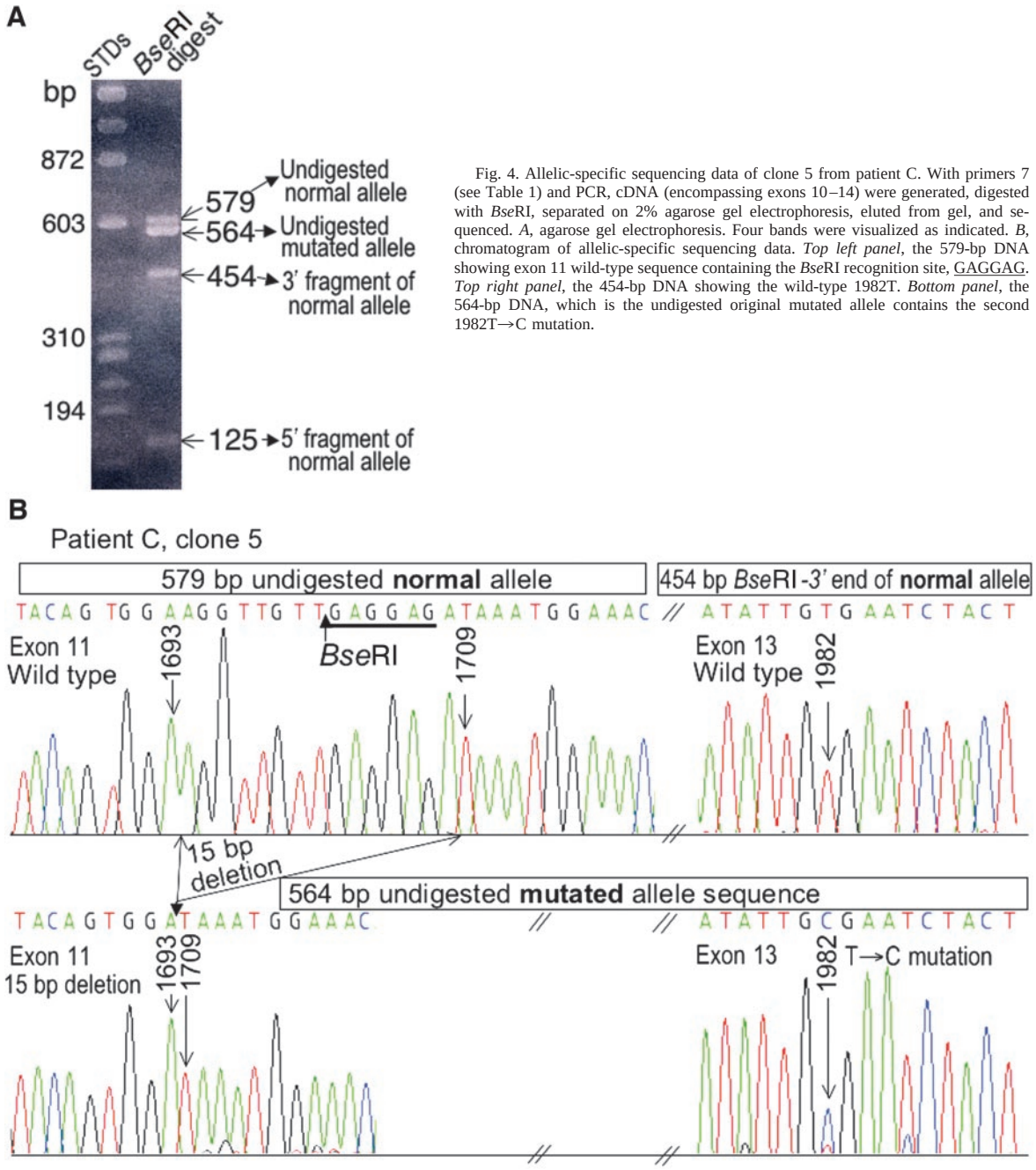

Fig. 4. Allelic-specific sequencing data of clone 5 from patient C. With primers 7 (see Table 1) and PCR, cDNA (encompassing exons 10–14) were generated, digested with *Bse*RI, separated on 2% agarose gel electrophoresis, eluted from gel, and sequenced. *A*, agarose gel electrophoresis. Four bands were visualized as indicated. *B*, chromatogram of allelic-specific sequencing data. *Top left panel*, the 579-bp DNA showing exon 11 wild-type sequence containing the *Bse*RI recognition site, GAGGAG. *Top right panel*, the 454-bp DNA showing the wild-type 1982T. *Bottom panel*, the 564-bp DNA, which is the undigested original mutated allele contains the second 1982T→C mutation.

reported with more than one mutation in *KIT*; therefore, finding a second and new *KIT* mutation in closely monitored imatinib-resistant clones is convincing *in vivo* evidence of a causal relationship. Allelic-specific sequencing analyses show that this novel *KIT* exon 13 missense mutation, 1982T→C, occurs in the original mutated allele, not in the normal allele. One possible explanation could be the local regional genetic instability of the allele that harbors an exon 11 or exon 9 mutation, predisposing it to a second hit of an additional mutation in the same allele. Under the selection pressure of imatinib treatment, the second possible explanation could be the preferential proliferative advantage of the clones that harbor the dominant activating exon 11 or exon 9 mutation plus second hit of 1982T→C mutation in the same allele, which may acquire substantially more advantage in imatinib resistance than those clones that harbor second hit of the 1982T→C mutation in the normal allele. These two possibilities are not mutually exclusive.

Val654 is in KIT kinase domain 1 and is conserved among ABL, src, hck, PDGFRα, and KIT. The crystal structure of KIT has recently been reported (17), but the coordinates are not yet available for us to construct the three-dimensional picture incorporating this new mutation. A schema (Fig. 3) showing the structural and functional regions of KIT is included as a reference. The first residue of the KIT ATP phosphate-binding loop (P-loop) is Gly596 (17, 18), which is 58 amino acids NH_2-terminal to this novel Val654Ala mutation. In close proximity to Val654Ala, are the imatinib contact points, Glu640, Thr670, Cys673, Asp810 (12, 13), and the ADP-binding residues Lys623, Glu671, and Cys673 (17). The conserved Glu640 in control helix (C-helix), a single α-helix, forms a critical interaction with the side chain of Lys623, which binds ADP. By structural analysis, this new mutation, Val654Ala, therefore, most likely produces allosteric conformational changes that alter the configuration of KIT kinase domain and the relative affinity of KIT to imatinib.

Kinase domain mutations in ABL in leukemia have almost always been associated with imatinib resistance (18-20). Some of the ABL mutations that confer imatinib resistance in leukemia were found to be present in leukemia patients before imatinib treatment (20). The novel mutation Val654Ala, which has never been reported in literature before, was not detectable in any pre-imatinib GISTs or any quiescent implants by routine PCR (Table 1, with primer 3 for genomic DNA and primer 7 for cDNA sequence), which indicates that the mechanism of imatinib resistance in clones 1, 2, 4, 5, 8, and 11 in patients A to E is due to either the development of a new mutation or the imatinib selection of an extremely low level of preexisting clones that harbor this mutation before treatment.

Because GISTs are initiated by constitutive KIT signal, KIT is an ideal target for therapy as evidenced by the dramatic and immediate effect of imatinib (Fig. 1*a-1* to *a-4*, *a-7*, *a-8*, *b-1*, *b-2*, *c-1*, *c-2*, *d-1*, *d-2*). For the same reason, it is also conceivable that a single missense mutation in kinase domain in KIT is sufficient to result in imatinib resistance and unleash the proliferative constraints. The 12 GIST patients presented in Table 2 underwent surgery at different times spanned over 24 months, and nucleotide sequence analyses were done shortly after each surgery at different times; hence, cross-contamination is unlikely. In addition, we obtained different exon 11 mutations in patients A–D and J–L, which provides direct proof against any cross-contamination. We anticipate that more new mutations will occur at the same or different KIT kinase domains and that other alternative mechanisms of imatinib resistance will be discovered.

Acknowledgments

We thank Dr. Waun K. Hong for support and funding from the Division of Cancer Medicine, Dr. Stanley Hamilton for helpful discussions, and Dr. Harry L. Evans for assistance in pathology, the DNA Sequencing Core Facility and Tissue Procurement and Banking Facility at University of Texas, M. D. Anderson Cancer Center and Goodwin Foundation. We thank Lynda J. Corley for laboratory assistance, Patricia A. Gabler and Dorothy J. Taylor for manuscript preparation, and Terasa A. Simmons for clinical data preparation.

References

1. Hirota S, Isozaki K, Moriyama Y, et al. Gain-of-function mutations of c-kit in human gastrointestinal stromal tumors. Science (Wash DC) 1998;279:577–80.
2. Koh JS, Trent JC, Chen LL, et al. Gastrointestinal stromal tumors: Overview of pathologic features, molecular biology, and therapy with imatinib mesylate. Histol Histopathol 2004;19:565–74.
3. Heinrich MC, Corless CL, Demetri GD, et al. Kinase mutations and imatinib response in patients with metastatic gastrointestinal stromal tumor. J Clin Oncol 2003;21:4342–9.
4. Allander SV, Nupponen NN, Ringnér M, et al. Gastrointestinal stromal tumors with KIT mutations exhibit a remarkably homogeneous gene expression profile. Cancer Res 2001;61:8624–8.
5. Sommer G, Agosti V, Ehlers I, et al. Gastrointestinal stromal tumors in a mouse model by targeted mutation of the Kit receptor tyrosine kinase. Proc Natl Acad Sci USA 2003;100:6706–11.
6. Ma Y, Cunningham ME, Wang X, Ghosh I, Regan L, Longley BJ. Inhibition of spontaneous receptor phosphorylation by residues in a putative α-helix in the KIT intracellular juxtamembrane region. J Biol Chem 1999;274:13399–402.
7. Chan PM, Ilangumaran S, La Rose J, Chakrabartty A, Rottapel R. Autoinhibition of the Kit receptor tyrosine kinase by the cytosolic juxtamembrane region. Mol Cell Biol 2003;23:3067–78.
8. Kinoshita K, Isozaki K, Hirota S, et al. C-kit Gene mutation at exon 17 or 13 is very rare in sporadic gastrointestinal stromal tumors. J Gastroenterol Hepatol 2003;18:147–51.
9. Hirota S, Nishida T, Isozaki K, et al. Familial gastrointestinal stromal tumors associated with dysphagia and novel type germline mutation of kit gene. Gastroenterology 2002;122:1493–99.
10. Heinrich MC, Corless CL, Deunsing A, et al. PDGFRA activating mutations in gastrointestinal stromal tumors. Science (Wash DC) 2003;299:708–10.
11. Hirota S, Ohashi A, Nishida T, et al. Gain-of-function mutations of platelet-derived growth factor receptor α gene in gastrointestinal stromal tumors. Gastroenterology 2003;125:660–7.
12. Fabbro D, Ruetz S, Buchdunger E, et al. Protein kinases as targets for anticancer agents: from inhibitors to useful drugs. Pharmacol Ther 2002;93:79–98.
13. Manley PW, Cowan-Jacob SW, Buchdunger E, et al. Imatinib: a selective tyrosine kinase inhibitor. Eur J Cancer 2002;38:S19–27.
14. Demetri GD, von Mehren M, Blanke CD, et al. Efficacy and safety of imatinib mesylate in advanced gastrointestinal stromal tumors. N Engl J Med 2002;347:472–480.
15. Kitamura Y, Hirota S, Nishida T. Gastrointestinal stromal tumors (GIST): A model for molecule-based diagnosis and treatment of solid tumors. Cancer Sci 2003;94:315–20.
16. Crosier PS, Ricciardi ST, Hall LR, Vitas MR, Clark SC, Crosier KE. Expression of isoforms of the human receptor tyrosine kinase c-kit in leukemic cell lines and acute myeloid leukemia. Blood 1993;82:1151–8.
17. Mol CD, Lim KB, Sridhar V, et al. Structure of c-kit product complex reveals the basis for kinase transactivation. J Biol Chem 2003;278:31461–4.
18. Azam M, Latek RR, Daley GQ. Mechanisms of autoinhibition and STI571/imatinib resistance revealed by mutagenesis of BCR-ABL. Cell 2003;112:831–43.
19. Gorre ME, Mohammed M, Ellwood K, et al. Clinical resistance to STI-571 cancer therapy caused by BCR-ABL gene mutation or amplification. Science (Wash DC) 2001;293:876–80.
20. Roche-Lestienne C, Soenen-Comu V, Grardel-Duflos N, et al. Several types of mutations of the Abl gene can be found in chronic myeloid leukemia patients resistant to ST1571, and they can pre-exist to the onset of treatment. Blood 2002;100:1014–8.

A Missense Mutation in KIT Kinase Domain 1 Correlates with Imatinib Resistance in Gastrointestinal Stromal Tumors

Lei L. Chen, Jonathan C. Trent, Elsie F. Wu, et al.

Cancer Res 2004;64:5913-5919.